Revisiting carbonate quantification in apatite (bio)minerals: a validated FTIR methodology

Anne Grunenwald, Christine Keyser, Anne-Marie Sautereau, Eric Crubézy, Bertrand Ludes, Christophe Drouet

Revisiting carbonate quantification in apatite (bio)minerals: a validated FTIR methodology

A. Grunenwald [a, b], C. Keyser [b], A.M. Sautereau [a], E. Crubézy [c], B. Ludes [b], C. Drouet [a, *]

[a] CIRIMAT Carnot Institute – Phosphates, Pharmacotechnics, Biomaterials, University of Toulouse, CNRS/INPT/UPS, ENSIACET, 4 allée Emile Monso, 31432 Toulouse Cedex 4, France
[b] Institute of Legal Medicine, AMIS Laboratory, CNRS UMR 5288, University of Strasbourg, 11 rue Humann, 67085 Strasbourg Cedex, France
[c] Molecular Anthropology and Image Synthesis Laboratory (AMIS), CNRS UMR 5288, University of Toulouse, 37 allée Jules Guesde, 31000 Toulouse, France

Keywords:
Carbonate
Apatite
Bone
FTIR
Diagenesis

A B S T R A C T

Carbonated apatites represent an important class of compounds encountered in many fields including anthropology, archeology, geology, medicine and biomaterials engineering. They constitute, in particular, the mineral part of bones and teeth, are found in sedimentary settings, and are used as biomimetic compounds for the development of bone tissue engineering scaffolds. Whether for assessing the degree of biomimetism of synthetic apatites or for better understanding diagenetic events, their thorough physico-chemical characterization is essential, and includes, in particular, the evaluation of their carbonate content. FTIR is especially well-suited for such a goal, as this spectroscopy technique requires only a low amount of specimen to analyze, and carbonate ions exhibit a clear vibrational signature. In this contribution, we critically discuss several FTIR-approaches that may be (or have been) considered in view of carbonation quantification. The best methodology appears to be based on the analysis of the $\nu_3(CO_3)$ and $\nu_1\nu_3(PO_4)$ modes. The area ratio $r_{c/p}$ between these two contributions was found to be directly correlated to the carbonate content of the samples ($R^2 = 0.985$), with the relation wt.% $CO_3 = 28.62^{*}r_{c/p} + 0.0843$. The method was validated thanks to titrations by coulometry assays for various synthetic reference samples exhibiting carbonate contents between 3 and 7 wt.%. The FTIR carbonate quantification methodology that we propose here was also tested with success on three skeletal specimens (two bones/one tooth), after elimination of the collagen contribution. Comparative data analysis is also presented, showing that the use of other vibration bands, or only peak heights (instead of peak areas), leads to significantly lower correlation agreement. This FTIR data treatment methodology is recommended so as to limit errors on the evaluation of carbonate contents in apatite substrates.

1. Introduction

Hard tissues (bones and teeth) in vertebrates are natural composite materials (Price et al., 1985) consisting of well-organized organic and inorganic moieties in tridimensional arrangements (Gomez-Morales et al., 2013; Landis et al., 1996), in order to fulfill appropriately physicochemical, biological, and mechanical functions. The mineral part is composed of an apatite phase that derives from hydroxyapatite (HA), $Ca_{10}(PO_4)_6(OH)_2$. In the case of enamel, the chemical composition of the apatite phase closely resembles that of HA (in a microcrystalline setting), whereas the apatite phase constituting bone mineral or dentin is clearly nanocrystalline and significantly departs from stoichiometry. In all cases, trace elements can also enter the structure, such as fluorine, magnesium or strontium among others (Elliott, 1994). These considerations typically illustrate the exceptional capacity of the apatite structure to adapt its composition and crystal dimensions to the functions that it has to achieve *in vivo* (low solubility, resistance to acidic attacks for enamel; greater solubility for bone mineral which has to undergo remodeling processes and remain active in homeostasis).

In all cases, carbonate ions are also found to substitute anions in biological apatites (Rey et al., 1989; Pasteris et al., 2014; Shimoda et al., 1990; Gomez-Morales et al., 2013; Elliott et al., 1985): phosphates (leading to "B-type" carbonated apatites) or hydroxides ("A-type"), or the mixed "AB-type". The incidence of carbonation in biological apatites is not anecdotic: carbonate ions, CO_3^{2-}, are

* Corresponding author. CIRIMAT Carnot Institute, ENSIACET, 4 allée Emile Monso, 31432 Toulouse cedex 4, France. Tel.: +33 (0)34 32 34 11; fax: +33 (0)34 32 34 99.
E-mail address: christophe.drouet@ensiacet.fr (C. Drouet).

known to be growth inhibitors for the apatitic structure (Shimoda et al., 1990); their presence is thus expected to modulate mineralization processes. Also, carbonate ions are thought to stabilize the non-apatitic surface layer present on apatite nanocrystals. Indeed, for a similar maturation time in solution, carbonated apatites exhibit a lower degree of maturity than their non-carbonated counterparts (internal communication). The presence of carbonate ions during the mineralization of collagenic proteins *in vivo* is thus likely to influence the final characteristics of the apatite crystals that are being formed, although the level of carbonation is known to increase with the maturity of the biomineral (Pellegrino and Biltz, 1972; Legros et al., 1987).

It is possible to prepare by soft chemical route some "biomimetic" apatite nanocrystals approaching the composition, structure, and microstructure of biological apatites, and their physico-chemical features can be tailored by controlling adequately the precipitation conditions (Vandecandelaere et al., 2012). Biomimetic analogs can be either precipitated in the presence or in the absence of carbonate ions. Recently, we highlighted some of the similarities existing between a carbonated apatite matured for one week (Grunenwald et al., 2014) and a typical modern bone specimen. Such synthetic apatite compounds can be considered as "models" of the mineral part of bones, allowing one to investigate interfacial phenomena in a simplified and more controlled way than with biologically-derived samples, as we did recently in the field of ancient DNA preservation (Grunenwald et al., 2014). Synthetic carbonated apatites are also good candidates for the setup of scaffolds for bone tissue engineering or for coating prosthetic devices, taking into consideration their intrinsic biocompatibility and similarity to bone mineral.

Whether of natural origin or of synthetic nature, carbonated apatites can be encountered in various fields of interest, from anthropology or forensic sciences (analysis of skeletal remains) to biomaterials engineering, as well as fundamental research aiming at better understanding biomineralization processes. In all cases, sample characterization is a necessary step, which includes the determination of the carbonation content. As regards synthetic samples, this determination is necessary to evaluate the degree of analogy (biomimetism) to bone mineral with varying maturity stages after bone remodeling. The CO_3 content in apatite compounds progressively increases upon maturation of the crystals (Pellegrino and Biltz, 1972). In the case of biological apatites, the knowledge of the carbonation level may help understanding diagenetic phenomena since the alteration of the CO_3 content from skeletal specimens appears to be site-specific (Trueman et al., 2008; Cazalbou et al., 2004; Kohn et al., 1999). Also, Roche et al. argued for changes to the A-B ratio in fossils compared to modern tissues, thus pointing out that the carbonate component of biogenic phosphates can change during diagenesis (Roche et al., 2010). In geochemistry and paleoenvironment/paleobiology domains, it may help to extract precious information via isotopic titrations of carbon or oxygen isotopes contained in the CO_3^{2-} anions (Suarez and Kohn, 2011; Lecuyer et al., 2010; Sponheimer and Lee-Thorp, 2001; Kohn et al., 1996; Tütken and Vennemann, 2011; Price et al., 1985).

The list of techniques that may potentially come into play for assessing the amount of carbonate ions associated with the apatite phase is however quite limited. Methods based on total carbon titration after sample calcination are generally associated with non-negligible uncertainties (estimated to several weight percent), which limits their practical usefulness. Methods based on the release of carbon dioxide upon acidification and subsequent electrochemical quantification (coulometry assays) yield significantly more accurate results (Eichert et al., 2007; Engleman et al., 1985), but require a substantial amount of sample (typically of the order of several tens to hundreds of milligrams) which is not often an option in the case of archeological or forensic specimens where only a very limited quantity of matter is available.

In this context, the use of vibrational spectroscopies such as Raman or Fourier Transform Infrared (FTIR) spectroscopies appears particularly relevant due to the high sensitivity of these techniques and the very low amount of specimen that they require (typically 1–2 mg). Lebon et al. have pointed out however some difficulties related to the use of Raman spectroscopy due to fluorescence of biological/fossil systems as well as to the low intensity of the carbonate contribution (Lebon et al., 2011). The $\nu_2(CO_3)$ and $\nu_3(CO_3)$ vibration modes of carbonate ions incorporated in an apatitic lattice are on the contrary quite easily detectable by FTIR. This technique thus appears as a potentially adapted technique for carbonation quantification. Puceat et al. proposed to follow, by FTIR, the carbonation of apatites on the basis of the ratio of peak heights between the 1415 cm^{-1} band of the $\nu_3(CO_3)$ band, mostly assignable to B-type carbonate, and the sum of the two peaks (i.e. 601 and 560 cm^{-1}) of the $\nu_4(PO_4)$ contribution (Puceat et al., 2004). In a rather similar intention, Featherstone et al. had previously investigated a method based on the ratio of extinction coefficients at 1415 and 575 cm^{-1} (Featherstone et al., 1984). However, this method based on a comparison of peak heights at selected wavenumbers can hardly account for the variability of carbonate chemical environments in all apatite specimens, where not only B-type carbonates but also A-type or even labile carbonates (pertaining to the non-apatitic surface layer on apatite nanocrystals (Gomez-Morales et al., 2013; Eichert et al., 2007; Rey et al., 2011)) may coexist in variable proportions (Rey et al., 2011). Moreover, the hydroxylation of apatite – which may be variable depending on stoichiometry – leads to a libration band at 632 cm^{-1} superimposed to the $\nu_4(PO_4)$ band (Drouet, 2013). It has also been suggested (Puceat et al., 2004; Sosa et al., 2013; Boskey et al., 2005) evaluating the carbonate contribution using the area or intensity ratio of the 1415 cm^{-1} band alone (not considering the rest of the $\nu_3(CO_3)$ contribution) relative to the $\nu_3(PO_4)$ phosphate band, instead of $\nu_4(PO_4)$, or exploiting the $\nu_2(CO_3)$, for example, through the $\nu_2(CO_3)/\nu_3\nu_1(PO_4)$ area ratio. However, in the case of HPO_4-containing apatites, the occurrence of overlapping HPO_4-related contributions in the $\nu_2(CO_3)$ domain adds some obvious complexity in IR data which does not seem to have received attention so far. Yet, most synthetic apatites obtained by wet chemistry as well as biological bone or dentin specimens are expected to be non-stoichiometric and to incorporate non-negligible proportions of HPO_4^{2-} ions (Gomez-Morales et al., 2013), the presence of which has thus to be considered prior to developing IR methodologies.

In this context, the present contribution intends to 1) discuss which carbonate and phosphate vibrational contributions should be favored in view of carbonation quantification, and 2) to develop and test an FTIR-based methodology adapted to the evaluation of the CO_3 content of both synthetic and biological specimens. The validation of the method has been made through the use of direct carbonate titrations via coulometry assays. To this end, we have prepared a set of carbonated apatite reference compounds to be used for calibration purposes, allowing us to check relationships between IR data (integrated intensities of several vibrational contributions) and coulometric results. The skeletal specimens tested in this work arose, on the contrary, from archeological settings.

2. Materials and methods

2.1. Synthetic apatite compounds

Several synthetic carbonated apatite samples, used as reference materials in this work, were synthesized by precipitation in aqueous medium, at close-to-physiological pH (experimental

value ~ 7.2) and at different temperatures, namely 10 °C, 20 °C, room temperature (22 °C), 37 °C, 50 °C, and 70 °C. Except for experiments run at room temperature or at 70 °C, the temperature was controlled using a double-envelope reactor and a circulating device allowing the recirculation of a fluid between the two envelopes for precise temperature regulation. The sample prepared at 70 °C could not be stabilized in the same way due to the inadequacy of using the recirculating device at this temperature. For this sample, the precipitation was undergone in an Erlenmeyer flask connected to a reflux condenser to avoid water evaporation.

Two solutions, A and B, were prepared prior to the precipitation. A calcium-containing solution (solution A, typically 75 ml) was prepared by dissolving $Ca(NO_3)_2 4H_2O$ (Merck Emsure grade, purity ≥99.0%) in deionized water, up to reaching the concentration of 0.3 M. In parallel, solution B (150 ml) containing a phosphate source and a carbonate source was prepared by dissolving $(NH_4)_2HPO_4$ (VWR Normapur grade, purity ≥99.0%) and $NaHCO_3$ (purity ≥99.0%) up to the respective concentrations of 0.45 M and 0.71 M. Solutions A and B were then mixed and allowed to mature in the mother solution, with or without magnetic stirring (as indicated in the text), for a maturation time varying between 0 and 15 days (aging time in solution). The precipitating medium was then filtered on Büchner funnel, thoroughly washed with deionized water and freeze-dried (freeze-dryer set to −80 °C and residual pressure 10 mbar). The freeze-dried powders were collected and stored in a freezer at −18 °C, to avoid any subsequent evolution prior to physico-chemical analyses.

These synthetic reference samples will be named "hacXX-Yd", where XX corresponds to the synthesis temperature (in degrees Celsius) and Y denotes the number of maturation days in solution prior to filtration.

2.2. Skeletal specimens

Three skeletal specimens, corresponding to various geographical areas and epochs (Iron Age, Middle Ages and twentieth century) were investigated. The samples were provided by the AMIS laboratory (CNRS, UMR 5288, France). The specimens will be identified, in the present work, using the following names: "20th Cent", "mid-ages", and "Iron age". The first sample, "20th Cent", corresponds to an adult male femur dating from the mid-twentieth century. The second, "mid-ages", is part of an adult male tooth originating from Roeschwoog Alsace, France, and dating from the Middle Ages (registry ref. #R3189B); this sample was obtained by crushing the entire tooth, thus mixing dentin and enamel. The third specimen, "Iron age", comes from the Iron Age period (around 1800–1400 BC) and corresponds to a female bone from Krasnoyarsk region, Russia (registry ref. #S09).

No chemical pretreatment was performed so as to limit possible alterations of the mineral part contained in the samples. The specimens were first roughly ground using a 6870 SamplePrep Freezer Mills (Fischer Bioblock, Illkirch, France) and then subjected to a milling process (Spex 5010 Freezer Mill) for the obtainment of fine powders in view of physico–chemical characterizations.

2.3. Physico–chemical characterization

Powder X-ray diffraction was used to confirm the apatitic nature of the crystallized phase contained in the samples (as well as the absence of secondary deposits such as calcite in the case of fossil bones/teeth). The XRD analyses were carried out on an INEL CPS 120 curved-counter diffractometer using the monochromatic Cobalt Kα radiation ($\lambda_{Co} = 1.78892$ Å).

The carbonate content of reference synthetic apatites was measured by coulometry using a CO_2 coulometer (UIC, Inc. CM 5014 coulometer) measuring in a closed system the carbon dioxide (CO_2) released during sample dissolution in acidic conditions (CM 5130 acidification unit, use of $HClO_4$ 2 M for synthetic samples and 6 M for biological specimens). The CO_2 released was automatically transferred into a photometric cell and titrated through an acid–base reaction (Engleman et al., 1985; Huffman, 1977). Barium carbonate (Prolabo, purity >99%) was used as a reference material for checking the calibration of the apparatus. Measures were made at least in duplicate. The uncertainty of this method is evaluated to ±0.5 wt.% CO_3.

Fourier Transform Infrared spectroscopy (FTIR), using KBr as a solid diluent, was used to analyze vibrational features of the specimens. About 1.5 mg of each sample was mixed and ground with 200 mg of KBr. Composite pellets were prepared out of this mixture by uniaxial compression under 8 tons cm^{-1} for *ca.* 10 s. The FTIR spectra were acquired by transmission, in the wavenumber range 400–4000 cm^{-1} using a Nicolet 5700 spectrometer (64 scans, with a resolution of 4 cm^{-1}). The spectra were subsequently analyzed with the OMNIC 8 software (Thermo Nicolet). Background deviations on FTIR spectra were corrected using the automatic background correction tool of the software (the background line consisting in a series of joint linear segments). This led to zeroing in particular the absorption levels at points such as 4000, ~2000, ~800 and 400 cm^{-1}. Fig. AR1 in the Additional Resources shows an example of spectrum (synthetic carbonated apatite) after background correction, in the 400–2000 cm^{-1} range.

Several analysis methodologies have been tested in this work for the reference samples, in view of seeking correlations between IR data (related to carbonate and phosphate species) and coulometry data. The different methodologies will be explained where adequate in the text; they essentially differ by the considered vibrational domains. In each case, the analytical reproducibility of intensity ratios was checked by performing the same quantification method in triplicate.

3. Results and discussion

3.1. Carbonated apatite reference compounds

The apatitic nature of the synthesized samples studied in this work has been verified by XRD analyses. In all cases a pattern typical of an apatitic phase was indeed detected, as attested in accordance to the JCPDS card no. 09-432 relative to hydroxyapatite. The typical pattern obtained relative to sample hac22-15d (i.e. prepared at T_{amb} ~22 °C and matured for 15 days) is reported in Fig. 1 as illustrative example, along with the indexation of the main diffraction lines.

The carbonation level of the reference samples (carbonated apatites prepared by precipitation in various conditions) was then evaluated by coulometry assays. A summary of the results obtained in terms of weight percent of carbonate associated with the apatite phase is given in Table 1. As may be remarked, for systems prepared in similar stirring conditions, the degree of carbonation of the apatite phase clearly rises upon increasing the synthesis temperature (comparing samples hac10-15d, hac20-15d, hac37-15d, hac50-15d) or the maturation time in solution (comparing samples hac22-0d, hac22-1d, hac22-15d). Note that the samples hac22-15d and hac70-15d (prepared respectively at 22 and 70 °C) display a lower carbonation level than what could be expected at first from the general temperature-driven tendency. Sample hac22-15d, however, cannot be directly compared with the other samples matured for 15 days, due to distinct stirring conditions; the absence of stirring potentially limiting the kinetics of carbonation (but being closer to "natural" conditions). The lower carbonation of sample hac70-15d is due to a different cause; it can be related to a temperature that

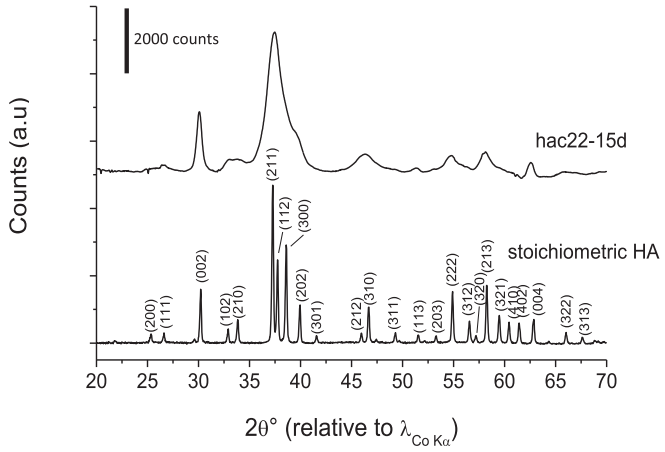

Fig. 1. Typical XRD pattern of the hac22-15d carbonated apatite sample, and indexation in reference to JCPDS card no. 09-432 relative to stoichiometric hydroxyapatite.

approaches the boiling temperature of the solution. In this respect, the elimination of dissolved gases (including CO_2) is facilitated.

These eight samples may be considered as a set of reference carbonated apatite samples, with a wide range of carbonation levels between 3 and 6.9 wt.% CO_3 (bone and teeth specimens being known to exhibit carbonate contents of up to about 4–8 wt.% CO_3, (Gomez-Morales et al., 2013; McElderry et al., 2013)).

3.2. FTIR data analysis for carbonated apatite reference compounds

Fig. 2 shows typical FTIR data found for such carbonated apatite reference materials; Fig. 2a gives an overview of the full spectra in the range 400–4000 cm^{-1}; and Fig. 2b reports an enlarged view of the range 400–1800 cm^{-1} where characteristic carbonate absorption corresponding to the $\nu_2(CO_3)$ and $\nu_3(CO_3)$ IR-active vibration modes can be evidenced respectively around 840–900 and 1350–1550 cm^{-1}. The former being less intense than the latter, Fig. 2c gives a zoomed view of the $\nu_2(CO_3)$ domain (which is merged with a vibrational contribution around 875 cm^{-1} assignable to HPO_4^{2-}). Finally, the attribution of each vibrational contribution is given in Fig. 2d in the typical case of sample hac37-15d. Apart from carbonation bands, the characteristic features of apatitic compounds are also clearly visible on these spectra, with apatitic hydroxide (OH^-_{ap}) bands at 3572 (O–H stretching) and 632 cm^{-1} (OH libration), as well as phosphate modes $\nu_1(PO_4)$, $\nu_2(PO_4)$, $\nu_3(PO_4)$, and $\nu_4(PO_4)$ as indicated in Fig. 2d. Water bands are also seen in the O–H stretching domain (3000–3600 cm^{-1}) as well as HOH deformation domain (1640 cm^{-1}).

As a general trend, it may be remarked that, upon increasing the maturation temperature from 10 to 70 °C, the resolution of the spectra is enhanced, with, in particular, an increasingly separated $\nu_1(PO_4)$ contribution from the $\nu_3(PO_4)$ domain. Also, the global amount of water associated with the samples progressively decreases. These observations may be related to an increased degree of crystallinity as can be expected from apatites precipitated in higher temperature conditions. This increase in crystallinity state has been investigated by analysis of the $\nu_4(PO_4)$ band (Fig. 3), by following two parameters as in Fig. 3b. First, the difference in position between the two maxima of this band was followed versus the maturation temperature, this parameter being related to the level of distortion existing in the PO_4 tetrahedrons. Second, a crystallinity index CI (aka "splitting factor") was evaluated from the "depth" of the pit between the two maxima using a method proposed in the literature (Shemesh, 1990; Weiner and Wagner, 1998; Thompson et al., 2011; Termine and Posner, 1966; Weiner and Bar-Yosef, 1990) and consisting of the ratio (after baseline correction) between the sum of the absorbance of the two maxima divided by the absorbance of the minimum between them. Despite non-negligible error bars, the two parameters conjointly suggest an evolution (decrease of splitting and increase of CI) toward better crystallized apatitic systems upon increasing the synthesis temperature, which confirms our above hypothesis. It may also be noted that the CI values were found here to range between *ca.* 3 and 4, which was also the case for pristine sedimentary apatites (Shemesh, 1990) as well as fossil or modern bones (Weiner and Wagner, 1998). Taking also into account the above-mentioned carbonation range of the reference compounds prepared here, the observations confirm that these compounds exhibit physico-chemical characteristics that are in perfect agreement with "target" unknown specimens susceptible to be analyzed (apatites from sediments, bones, synthetic analogs). These reference compounds thus appear as particularly relevant for the establishment of an FTIR methodology for carbonate quantification.

3.3. Selection of FTIR contributions to be considered for carbonate quantification

It is essential at this stage to discuss *which* FTIR contributions have to be considered in view of carbonation quantification. In order to inspect the degree of carbonation of a phosphate matrix, as is the case here, the follow-up of a ratio between a carbonate contribution (numerator) and a phosphate contribution (denominator) appears coherent. Numerous factors such as HPO_4:PO_4 ratio, A:B ratio of CO_3, labile surface CO_3, and lattice distortion from variable minor element chemistry all affect band position, shape, and intensity. Thus, an area-based method appears preferable to considering peak heights at selected wavenumbers.

3.3.1. Selection of carbonate contribution

As mentioned above, the presence of CO_3^{2-} ions leads to two vibration modes active in IR, namely $\nu_2(CO_3)$ and $\nu_3(CO_3)$ (Rey et al., 2011). However, the P–OH stretching vibration at 875 cm^{-1} of HPO_4^{2-} ions, that are also generally present in nonstoichiometric apatites, is superimposed with the $\nu_2(CO_3)$ mode which falls typically in the range 840–900 cm^{-1}. The consideration of this carbonate mode to assess the degree of carbonation of apatitic compounds thus becomes problematical. It may be attempted, via spectral decomposition, to separate each contribution arising in this spectral range, especially for removing the part linked to HPO_4. However, this task is made difficult by the possible presence of many contributions with maxima found to be rather close in position, including B-type and A-Type carbonates (respectively around 872 and 883 cm^{-1}, (Rey et al., 2011)), but also labile carbonates giving rise to a large band for which the exact position is

Table 1
Carbonation levels for the carbonated apatite references prepared in this work, and temperature control conditions.

Sample	hac22-0d	hac22-1d	hac10-15d	hac20-15d	hac22-15d	hac37-15d	hac50-15d	hac70-15d
Stirring	no	no	yes	yes	no	yes	yes	yes
Wt%. CO_3	3	3	5.9	5.9	*5.5*	6.8	6.9	*5.3*

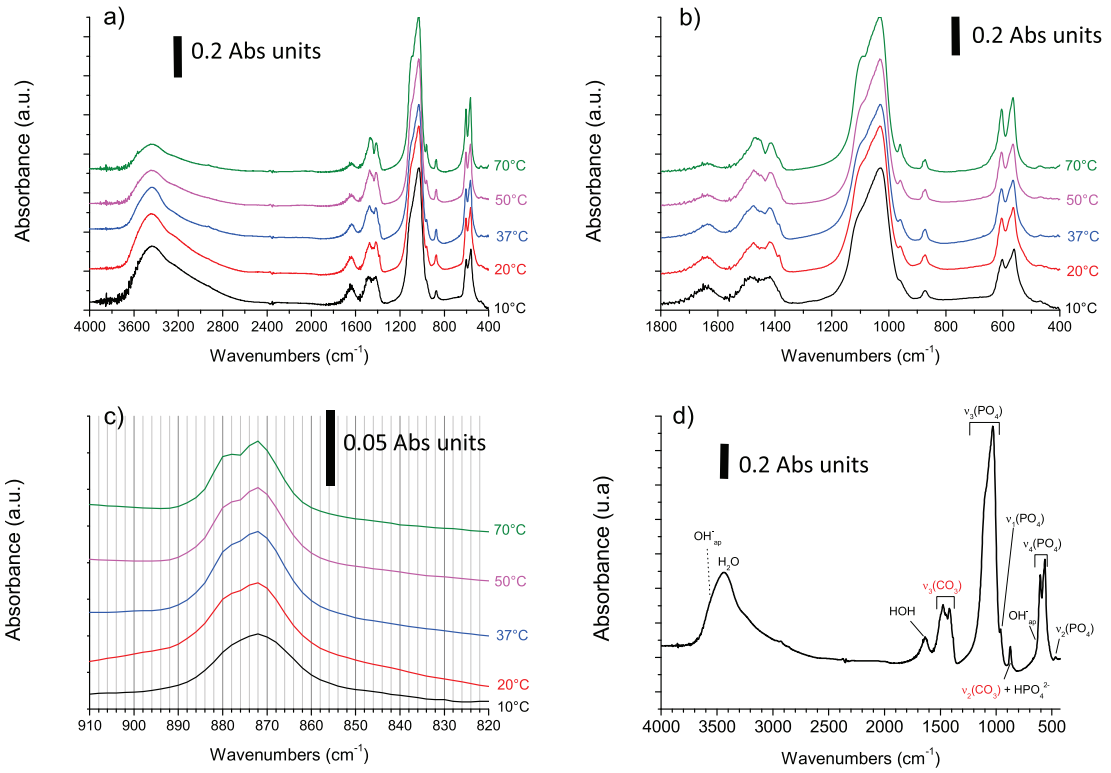

Fig. 2. FTIR spectra for carbonated apatite reference compoundss: a) typical spectra obtained for various maturation temperatures (for 15 days of maturation), b) zoom on the 400–1800 cm^{-1} range, c) detail on the $\nu_2(CO_3)$ region, d) indexation of bands (example of sample hac37-15d).

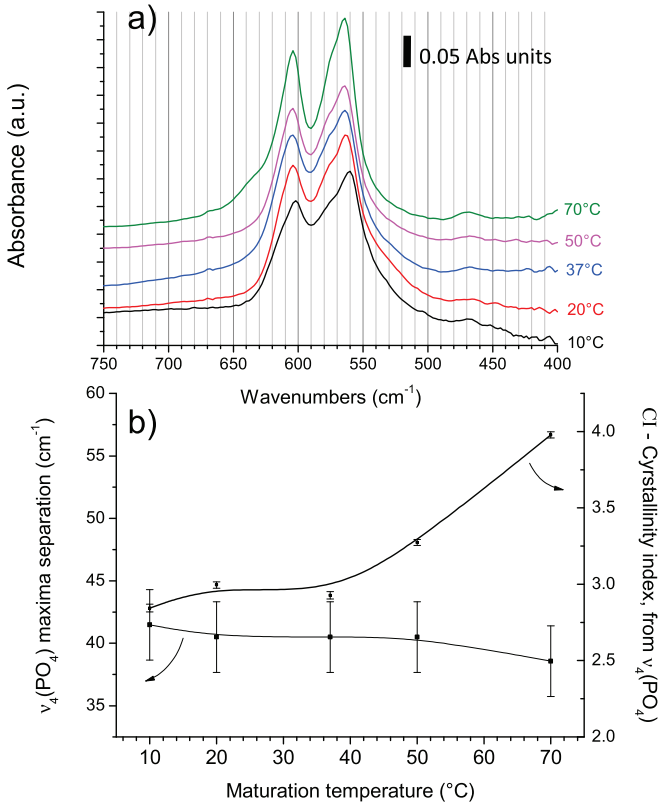

Fig. 3. Analysis of the $\nu_4(PO_4)$ vibrational domain for carbonated apatite references prepared at various temperatures: a) spectra in the 400–750 cm^{-1} range, and b) evolution of $\nu_4(PO_4)$ maxima separation and crystallinity index CI (or "splitting factor") evaluated from the $\nu_4(PO_4)$ domain.

not well-known (carbonation in amorphous calcium phosphate leading to absorption at 866 cm^{-1} (Rey et al., 2011)) as well as the HPO_4^{2-} contribution at 875 cm^{-1}. Moreover, the external titration of HPO_4^{2-} ions by methods such as thermogravimetry (TGA) or spectrophotometry (e.g. using the yellow phospho–vanado–molybdenum complex (Gee and Dietz, 1953)) is extremely delicate (Elliott, 1994) in the co-presence of carbonate ions due to parasite reactions such as $CO_3^{2-} + 2HPO_4^{2-} \rightarrow CO_2 + H_2O + 2PO_4^{3-}$. Therefore, the use of the $\nu_2(CO_3)$ does not appear appropriate for the evaluation of the carbonate content in a general situation where the presence of HPO_4^{2-} ions cannot be excluded.

In contrast, the $\nu_3(CO_3)$ vibration mode is well separated from the main phosphate absorption bands, which makes it suitable for carbonate quantification. In the case of biological specimens, however, a complication arises due to vibrations of collagen (Kimura-Suda et al., 2009), the amide bands of which lead to absorptions typically in the range 1930–1230 cm^{-1}. This superimposition of IR bands from carbonate and collagen therefore prevents a direct analysis of mineral carbonation. Chemical treatments aiming at dissolving the collagen matrix could also lead to modifications of the apatite features, and it is thus not advised. Since the added complexity is due to the presence of amide bands from collagen, it is, however, theoretically possible to subtract this contribution by subtracting – with an adequate multiplying factor (until minimizing the intensity of amide vibrations in the 1930–1230 cm^{-1} domain) – the spectrum of pure collagen acquired in the same experimental conditions. Consequently, whether for synthetic or biological apatitic samples, the evaluation of carbonation seems to be appreciable based on the analysis of the $\nu_3(CO_3)$ mode. This mode has thus been selected (see the following section for the experimental validation on both synthetic and biological specimens).

3.3.2. Selection of phosphate contribution

Phosphate ions lead to various FTIR contributions. However, since the $\nu_1(PO_4)$ and $\nu_2(PO_4)$ modes are only poorly active in infrared, considering them for quantification purposes would lead to increased uncertainties. In contrast, the $\nu_3(PO_4)$ and $\nu_4(PO_4)$ domains are significantly more intense, which is expected to limit propagated errors. The libration band of apatitic OH^- ions, however, appears at 632 cm^{-1}, which superimposes to the $\nu_4(PO_4)$ domain. Since apatite compounds are often nonstoichiometric due to the presence of vacancies in calcium and hydroxide sites, the level of hydroxylation may significantly vary from one sample to another, thus modifying the overall shape of the $\nu_4(PO_4)$ band. As this libration contribution can be non-negligible in intensity but also because it cannot easily be distinguished from the phosphate vibrations belonging to the $\nu_4(PO_4)$ domain (unless using time-consuming spectral decomposition methods), the exploration of the $\nu_4(PO_4)$ domain for in carbonate quantification methodology does not seem appropriate.

Overall, the $\nu_3(PO_4)$ appears the best choice to assess carbonate contents of apatite. However, especially in low-crystallinity samples, the $\nu_1(PO_4)$ singlet vibration is not cleanly separated from the $\nu_3(PO_4)$ band (e.g. Fig. 2b), and appears as a shoulder to $\nu_1(PO_4)$. Thus the combined $\nu_1\nu_3(PO_4)$ domain appears most practical in avoiding additional spectral treatment to subtract the $\nu_1(PO_4)$ contribution.

3.4. Exploration of FTIR methodologies

The vibrational domains retained for this carbonation analysis are $\nu_3(CO_3)$ for carbonate ions and $\nu_1\nu_3(PO_4)$ for phosphates. Based on our experimental IR spectra, we measured for each of the reference samples, using the OMNIC 8 software, the integrated intensities (=peak areas) corresponding to these three components. These measurements were carried out after a preliminary baseline correction of the complete 4000–400 cm^{-1} spectrum. The integration of the $\nu_3(CO_3)$ band was done in such a way as to include the totality of the $\nu_3(CO_3)$ contribution, typically between 1570 and 1330 cm^{-1}. The $\nu_1\nu_3(PO_4)$ contribution was integrated between 1230 and ~900 cm^{-1}. This lower limit was selected as the local minimum in order to avoid including the band expanding from *ca.* 800 to *ca.* 900 cm^{-1} due to $\nu_2(CO_3)$ and to HPO_4^{2-}. The upper limit of 1230 cm^{-1} was chosen because collagen subtraction for biological samples is bound to alter the region 1930–1230 cm^{-1} where amide bands are located (Boskey et al., 2005). The evaluation of the band area corresponding to $\nu_1\nu_3(PO_4)$ was found, in contrast, to be essentially unaffected (data not presented graphically here) by the collagen subtraction between these limits of 1230 and 900 cm^{-1}, therefore confirming the possibility of using this wavenumber range. The integration areas of interest for the determination of the carbonate/phosphate ratio denoted "$r_{c/p}$" between the integrated intensity of $\nu_3(CO_3)$ and that of $\nu_1\nu_3(PO_4)$ are shown graphically in Fig. 4a.

The evolution of the amount of carbonate in reference samples (as measured by coulometry) has been plotted in Fig. 4b versus the ratio $r_{c/p}$. Interestingly, a linear trend could be evidenced (see raw data on Table AR1 in the Additional Resources), with good correlation parameters ($R^2 = 0.985$), leading to the relationship given in Equation (1):

$$\text{wt.\% } CO_3 = 28.62 * r_{c/p} + 0.0843 \quad (1)$$

Despite absolute uncertainties on data points, this correlation confirms advantageously the possibility to exploit IR data for drawing quantitative assessments on the level of carbonation of apatitic compounds, and using the areas of the two spectral components $\nu_3(CO_3)$ and $\nu_1\nu_3(PO_4)$. The ordinate values (y-axis) given by this method are associated with an absolute error close to ±0.5% on the final wt.% CO_3. In this Figure, the fitted line was graphically prolonged (dashed line) down to 2 wt.% CO_3 and up to 13 wt.% CO_3 to access visually the correspondence between $r_{c/p}$ and wt.% CO_3 for a larger range of carbonation levels.

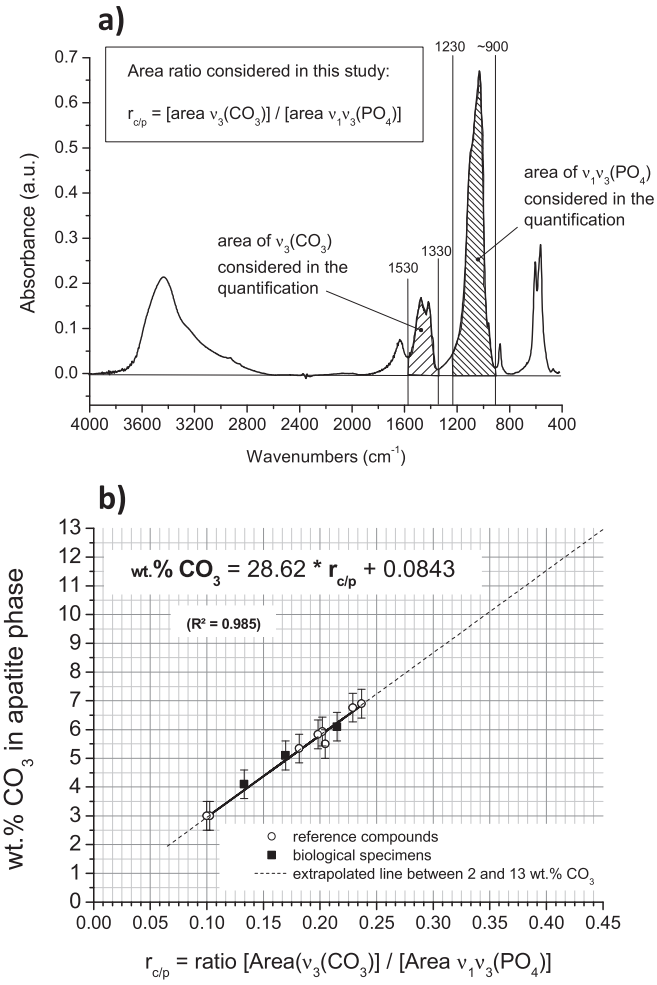

Fig. 4. FTIR methodology for carbonate quantification: a) evaluation of the ratio $r_{c/p}$ between the integrated intensity of $\nu_3(CO_3)$ and that of $\nu_1\nu_3(PO_4)$, and b) correlation between $r_{c/p}$ and the carbonation amount (in wt.% CO_3) in the apatite phase of synthetic reference compounds and for three biological samples.

If the same type of relationship is sought by considering the $\nu_4(PO_4)$ domain instead of $\nu_1\nu_3(PO_4)$, a poorer correlation is reached: when applied to reference samples from Table 1, a correlation coefficient of R^2 ~ 0.82 is found (see Fig. AR2 in the Additional Resources). This poor agreement was expected based on the above discussion (see previous section), because the level of hydroxylation of the apatite phase is bound to vary between samples, and the $\nu_{lib}(OH)$ libration band at 632 cm^{-1} cannot be easily separated from the large $\nu_4(PO_4)$ band, therefore generating a bias to the use of the $\nu_4(PO_4)$ band in the determination of a carbonation ratio.

If $r_{c/p}$ is calculated by considering the area of the $\nu_2(CO_3)$ band instead of $\nu_3(CO_3)$, an even poorer correlation is observed with the amount of carbonate of the reference compounds, with a coefficient of R^2 ~ 0.46 (Fig. AR2). Again, this illustrates the inadequacy mentioned in the previous section to inspect the carbonation level on the basis of the $\nu_2(CO_3)$ band, which in fact also contains a non-negligible and varying HPO_4 contribution among the samples.

As indicated in the introduction, the use of peak heights rather than areas has been proposed to follow the carbonation level of apatites, especially by considering the maximum at 1415 cm^{-1} (in the $\nu_3(CO_3)$ domain) relative to the phosphate maximum of the $\nu_3(PO_4)$ band, around 1040 cm^{-1} (exact position depending on the samples). Plotting the carbonate content measured by coulometry versus this height ratio led, when applied to the reference samples, to a correlation coefficient of R^2 ~0.76 (Fig. AR2). Although a rather linear trend can be observed here, the quality of this correlation remains lower than the one obtained using the $r_{c/p}$ area ratio (R^2 ~ 0.99).

All of these findings validate the $r_{c/p}$ area ratio between $\nu_3(CO_3)$ and $\nu_1\nu_3(PO_4)$ as the most adapted FTIR parameter to consider for carbonation quantification in apatites, this ratio being defined as the quotient between the full area of the $\nu_3(CO_3)$ band (typically in the range 1570–1330 cm^{-1}) and the area of the $\nu_1\nu_3(PO_4)$ band (typically in the range 900–1230 cm^{-1}).

At this point, it was interesting to check the validity of this $\%CO_3 = f(r_{c/p})$ relationship also for biological apatites. Three skeletal specimens (two from bones and one from a tooth), as described in the experimental section, were selected to this end. The absence of calcite as secondary deposit in these biological/fossil specimens was confirmed by XRD analyses as well as IR spectroscopy (absence of the calcite band at 712 cm^{-1}). In a first step, the carbonation of each of these three samples was directly measured by coulometry. This was made possible by the occurrence of enough bone/tooth matter for the selected specimens, as 50–80 mg of sample was needed in each coulometry experiment (performed at least in duplicate). As always for coulometry assays, a calibration was preliminarily done with barium carbonate ($BaCO_3$). Since skeletal specimens are also associated with an organic matrix, most of which is collagenic in nature, we also ran a test with a known quantity of $BaCO_3$ added with bovine collagen (type I from bovine Achilles tendon, Sigma Aldrich), 12 wt.% in proportion, in order to check whether the presence of this protein in the reacting cell could modify the response of the coulometer. Advantageously, no deviation of the apparatus outcome was pointed out, confirming that coulometry assays could also be run on biological specimens. Considering bone and tooth samples as containing respectively 20 and ~5% of organic matter, the coulometry results (obtained initially with 50–80 mg of bone/tooth specimen) could be corrected to derive the amount of carbonation relative to the mineral phase (apatite only) in these samples. This led to a carbonation level in the apatite phase contained in the biological samples "20th Cent", "mid-ages", and "Iron age" of wt.% CO_3 = 5.1, 4.1, and 6.1% (±0.5%), respectively.

In addition, FTIR spectra were collected for these three skeletal specimens, in the same conditions as was done above for synthetic reference compounds. Fig. 5 reports a typical example obtained for such biological specimens. Due to the presence of the organic matrix, the spectral signature of collagen appears clearly on the spectrum with amide bands distinguishable in the region of 1930–1230 cm^{-1}, thus partly overlapping with inorganic carbonate. In order to take into account, in the $\%CO_3 = f(r_{c/p})$ relationship, only the vibrational contribution of carbonate, a spectral treatment was carried out by subtracting a typical spectrum of type I bovine bone collagen (modern collagen from own collection; access to IR spectra for collagen with varying preservation states in link with diagenesis were not accessible to us) until minimizing the amide contributions in the above-cited region (Fig. 5). In practice, this subtraction of the collagen contribution thus consisted in increasing the multiplying factor "γ" in the global equation [corrected spectrum] = [initial spectrum] − γ*[collagen spectrum] until obtaining visually a negligible absorption for the amide contributions. This collagen subtraction resulted in spectra judged

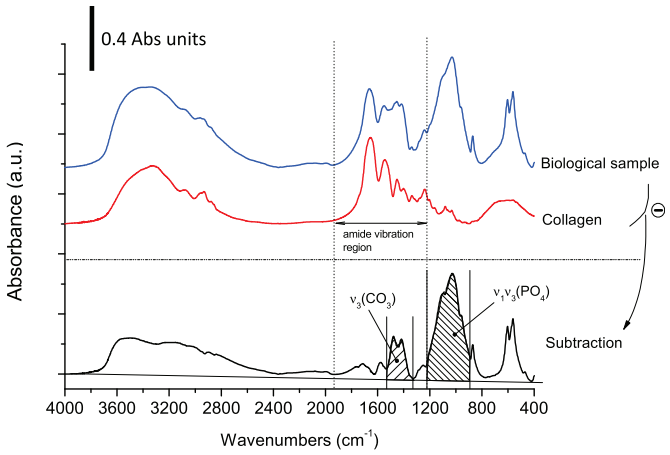

Fig. 5. Example of FTIR spectrum for biological specimen (case of Iron age bone sample) and for collagen (modern bovine bone collagen type I from own collection), and subtraction result (obtained by minimizing the intensity of amide vibrations in the 1930–1230 cm^{-1} domain).

satisfactory in terms of global appearance as compared with usual FTIR data recorded for synthetic carbonated apatites (see Fig. 2). Notably, the $\nu_1\nu_3(PO_4)$ domain was found to be only affected around the base of the absorption band without noticeable alteration of its general shape, thus making it potentially usable for quantification purposes. It may be noted that non-collagenous residues may also be present in biological/fossil specimens, however their amounts remain limited as compared to that of collagen. By analyzing by FTIR the organic residue found after acidic dissolution of the apatite mineral, we confirmed for the samples studied here that collagen was main organic component, and that non-collagenous matter led to very minor modifications of the 1530–1330 cm^{-1} carbonate domain (Fig. AR3 in the Additional Resources).

After collagen subtraction, the integrated intensities of the full $\nu_3(CO_3)$ domain (range 1530–1330 cm^{-1}) and of the $\nu_3\nu_1(PO_4)$ band (between 1230 and 890 cm^{-1}) were measured as done previously for synthetic samples, allowing us to derive the corresponding $r_{c/p}$ ratios. The application of Equation (1) to these data led to the respective carbonate contents of 4.9 ± 0.5, 3.9 ± 0.5 and 5.7 ± 0.5%, for samples "20th Cent", "mid-ages", and "Iron age" (to be compared with 5.1 ± 0.5, 4.1 ± 0.5 and 6.1 ± 0.5). A good agreement is, therefore, found between estimated carbonate contents calculated from Equation (1) and coulometric data for these biological samples. The three datapoints corresponding to these biological specimens have been added to the $\%CO_3 = f(r_{c/p})$ plot in Fig. 4b, which shows graphically that the IR-based methodology described in this paper for the quantification of carbonation of apatite phases is also applicable to skeletal specimens, provided that the vibrational contribution of collagen is preliminarily subtracted.

4. Concluding statements

The question of carbonate quantification in apatitic compounds, whether of synthetic or biological origin, is relevant for many reasons. In synthetic systems, the determination of the level of carbonation allows to draw conclusions relative to the degree of "biomimetism" of the sample, for example, as compared with mature or newly-formed bone matter. The presence of carbonation ions can clearly influence crystallization processes and these ions may also stabilize the non-apatitic surface layer on apatitic nanocrystals. Synthetic carbonated apatites could also serve as reference materials in view of the establishment of calibration curves, for example, in relation to biogenic phosphates that may have been

formed at various temperatures. In this contribution, we noted the direct effect of synthesis temperature on the level of carbonation and on other parameters such as crystallinity, evidenced on the basis of FTIR spectral analysis. In the case of skeletal specimens, the exploration of the carbonate content is of prime importance for characterizing these samples and drawing conclusions on biomineralization, diagenetic evolutions, paleoecology, etc., especially by exploiting ^{13}C and ^{18}O isotopic responses.

In this contribution, based on FTIR data, we discussed which carbonate and phosphate vibrations bands appear the most appropriate for carbonation quantification. We then developed and tested a quantification methodology based on an area ratio between the $\nu_3(CO_3)$ band and the $\nu_1\nu_3(PO_4)$ contribution, with integration limits that have been defined. We also checked this methodology quantitatively in comparison with direct coulometry measurements performed both on synthetic reference samples ($R^2 = 0.985$) and biological/fossil specimens, pointing out a good overall correlation. The absence of carbonated secondary deposits such as calcite should be verified for fossil specimens, for instance on the basis of XRD and/or IR analyses (e.g. absence of sharp band at 712 cm^{-1}).

The obtained relationship, expressed by Equation (1) (wt.% $CO_3 = 28.62^{*}r_{c/p} + 0.0843$), is intended to serve in the future for more systematic and comparable studies dedicated to carbonated apatites, whether of synthetic or natural origin.

Acknowledgments

This research was supported in part by the Institute of Ecology and Environment (INEE) and the Institute of Chemistry (INC) of the French National Center for Scientific Research (CNRS).

Appendix A. Supplementary data

Supplementary data related to this article can be found at http://dx.doi.org/10.1016/j.jas.2014.05.004.

References

Boskey, A.L., DiCarlo, E., Paschalis, E., West, P., Mendelsohn, R., 2005. Comparison of mineral quality and quantity in iliac crest biopsies from high- and low-turnover osteoporosis: an FT-IR microspectroscopic investigation. Osteoporos. Int. 16 (12), 2031–2038.

Cazalbou, S., Eichert, D., Drouet, C., Combes, C., Rey, C., 2004. Biological mineralisations based on calcium phosphate. Comptes. Rendus. Palevol. 3 (6–7), 563–572.

Drouet, C., 2013. Apatite formation: why it may not work as planned, and how to conclusively identify apatite compounds. Biomed. Res. Int. 2013, 12 http://dx.doi.org/10.1155/2013/490946. Article ID 490946.

Eichert, D., Drouet, C., Sfihi, H., Rey, C., Combes, C., 2007. Nanocrystalline apatite-based biomaterials: synthesis, processing and characterization. In: Kendall, J.B. (Ed.), Biomaterials Research Advances. Nova Science Publishers, pp. 93–143.

Elliott, J.C., 1994. Structure and Chemistry of the Apatites and Other Calcium Orthophosphates, vol. 18. Elsevier Science, Amsterdam.

Elliott, J.C., Holcomb, D.W., Young, R.A., 1985. Infrared determination of the degree of substitution of hydroxyl by carbonate ions in human dental enamel. Calcif. Tissue Int. 37 (4), 372–375.

Engleman, E.E., Jackson, L.L., Norton, D.R., 1985. Determination of carbonate carbon in geological materials by coulometric titration. Chem. Geol. 53 (1–2), 125–128.

Featherstone, J.D.B., Pearson, S., Legeros, R.Z., 1984. An infrared method for quantification of carbonate in carbonated apatites. Caries Res. 18 (1), 63–66.

Gee, A., Dietz, V.R., 1953. Determination of phosphate by differential spectrophotometry. Ann. Chem. 25, 1320–1324.

Gomez-Morales, J., Iafisco, M., Manuel Delgado-Lopez, J., Sarda, S., Drouet, C., 2013. Progress on the preparation of nanocrystalline apatites and surface characterization: overview of fundamental and applied aspects. Prog. Cryst. Growth Charact. Mater. 59 (1), 1–46.

Grunenwald, A., Keyser, C., Sautereau, A.M., Crubezy, E., Ludes, B., Drouet, C., 2014. Adsorption of DNA on biomimetic apatites: toward the understanding of the role of bone and tooth mineral on the preservation of ancient DNA. Appl. Surf. Sci. 292, 867–875.

Huffman, E.W.D., 1977. Performance of a new automatic carbon-dioxide coulometer. Microchem. J. 22 (4), 567–573.

Kimura-Suda, H., Kajiwara, M., Matsumoto, N., Murayama, H., Yamato, H., 2009. Characterization of apatite and collagen in bone with FTIR imaging. Mol. Cryst. Liq. Cryst. 505, 302–307.

Kohn, M.J., Schoeninger, M.J., Barker, W.W., 1999. Altered states: effects of diagenesis on fossil tooth chemistry. Geochim. Et. Cosmochim. Acta 63 (18), 2737–2747.

Kohn, M.J., Schoeninger, M.J., Valley, J.W., 1996. Herbivore tooth oxygen isotope compositions: effects of diet and physiology. Geochim. Et. Cosmochim. Acta 60 (20), 3889–3896.

Landis, W.J., Hodgens, K.J., Arena, J., Song, M.J., McEwen, B.F., 1996. Structural relations between collagen and mineral in bone as determined by high voltage electron microscopic tomography. Microsc. Res. Tech. 33 (2), 192–202.

Lebon, M., Müller, K., Bellot-Gurlet, L., Paris, C., Reiche, I., 2011. Application des micro-spectrométries infrarouge et Raman à l'étude des processus diagénétiques altérant les ossements paléolithiques. ArchéoSciences 35, 179–190.

Lecuyer, C., Balter, V., Martineau, F., Fourel, F., Bernard, A., Amiot, R., Gardien, V., Otero, O., Legendre, S., Panczer, G., Simon, L., Martini, R., 2010. Oxygen isotope fractionation between apatite-bound carbonate and water determined from controlled experiments with synthetic apatites precipitated at 10-37 degrees C. Geochim. Et. Cosmochim. Acta 74 (7), 2072–2081.

Legros, R., Balmain, N., Bonel, G., 1987. Age-related changes in mineral of rat and bovine cortical bone. Calcif. Tissue Int. 41 (3), 137–144.

McElderry, J.D.P., Zhu, P.Z., Mroue, K.H., Xu, J.D., Pavan, B., Fang, M., Zhao, G.S., McNerny, E., Kohn, D.H., Franceschi, R.T., Holl, M.M.B., Tecklenburg, M.M.J., Ramamoorthy, A., Morris, M.D., 2013. Crystallinity and compositional changes in carbonated apatites: evidence from P-31 solid-state NMR, Raman, and AFM analysis. J. Solid State Chem. 206, 192–198.

Pasteris, J.D., Yoder, C.H., Wopenka, B., 2014. Molecular water in nominally unhydrated carbonated hydroxylapatite: the key to a better understanding of bone mineral. Am. Mineralogist 99 (1), 16–27.

Pellegrino, E.D., Biltz, R.M., 1972. Mineralization in the chick embryo. I. Monohydrogen phosphate and carbonate relationships during maturation of the bone crystal complex. Calcif. Tissue Res. 10 (2), 128–135.

Price, T.D., Schoeninger, M.J., Armelagos, G.J., 1985. Bone chemistry and past behavior – an overview. J. Hum. Evol. 14 (5), 419–447.

Puceat, E., Reynard, B., Lecuyer, C., 2004. Can crystallinity be used to determine the degree of chemical alteration of biogenic apatites? Chem. Geol. 205 (1–2), 83–97.

Rey, C., Collins, B., Goehl, T., Dickson, I.R., Glimcher, M.J., 1989. The carbonate environment in bone-mineral – a resolution enhanced Fourier-Transform Infrared-Spectroscopy study. Calcif. Tissue Int. 45 (3), 157–164.

Rey, C., Combes, C., Christophe, D., Grossin, D., 2011. Bioactive ceramics: physical chemistry. In: Ducheyne, P., Healy, K.E., Hutmacher, D.W., Grainger, D.W., Kirkpatrick, C.J. (Eds.), Comprehensive Biomaterials. Elsevier, pp. 187–221.

Roche, D., Segalen, L., Balan, E., Delattre, S., 2010. Preservation assessment of Miocene–Pliocene tooth enamel from Tugen Hills (Kenyan Rift Valley) through FTIR, chemical and stable-isotope analyses. J. Archaeol. Sci. 37 (7), 1690–1699.

Shemesh, A., 1990. Crystallinity and diagenesis of sedimentary apatites. Geochim. Cosmochim. Acta 54 (9), 2433–2438.

Shimoda, S., Aoba, T., Moreno, E.C., Miake, Y., 1990. Effect of solution composition on morphological and structural features of carbonated calcium apatites. J. Dent. Res. 69 (11), 1731–1740.

Sosa, C., Vispe, E., Nunez, C., Baeta, M., Casalod, Y., Bolea, M., Hedges, R.E.M., Martinez-Jarreta, B., 2013. Association between ancient bone preservation and DNA Yield: a multidisciplinary approach. Am. J. Phys. Anthropol. 151 (1), 102–109.

Sponheimer, M., Lee-Thorp, J.A., 2001. The oxygen isotope composition of mammalian enamel carbonate from Morea Estate, South Africa. Oecologia 126 (2), 153–157.

Suarez, C., Kohn, M., 2011. Does carbonate content of biogenic apatite correlate with body temperature? J. Vertebrate Paleontol. 31, 201–201.

Termine, J.D., Posner, A.S., 1966. Infra-ref determination of the percentage of crystallinity in apatitic calcium phosphates. Nature 211, 268–270.

Thompson, T.J.U., Islam, M., Piduru, K., Marcel, A., 2011. An investigation into the internal and external variables acting on crystallinity index using Fourier Transform Infrared Spectroscopy on unaltered and burned bone. Palaeogeogr. Palaeoclimatol. Palaeoecol. 299 (1–2), 168–174.

Trueman, C.N., Privat, K., Field, J., 2008. Why do crystallinity values fail to predict the extent of diagenetic alteration of bone mineral? Palaeogeogr. Palaeoclimatol. Palaeoecol. 266 (3–4), 160–167.

Tütken, T., Vennemann, T.W., 2011. Fossil bones and teeth: preservation or alteration of biogenic compositions? Palaeogeogr. Palaeoclimatol. Palaeoecol. 310 (1–2), 1–8.

Vandecandelaere, N., Rey, C., Drouet, C., 2012. Biomimetic apatite-based biomaterials: on the critical impact of synthesis and post-synthesis parameters. J. Mater. Sci. Mater. Med. 23 (11), 2593–2606.

Weiner, S., Bar-Yosef, O., 1990. States of preservation of bones from prehistoric sites in the near east: a survey. J. Archaeol. Sci. 17 (2), 187–196.

Weiner, S., Wagner, H.D., 1998. The material bone: structure mechanical function relations. Annu. Rev. Mater. Sci. 28, 271–298.